Scientific African 14 (2021) e01025

Contents lists available at ScienceDirect

Scientific African

journal homepage: www.elsevier.com/locate/sciaf

Atherogenic index and lipid profiles in albino rats fed with surface modified *Hibiscus sabdariffa* cellulose

Adewale Adewuyi[a,*], Chiagoziem A. Otuechere[b], Olusegun L Adebayo[b], Mmachukwu Oyeka[b], Caleb Adewole[b]

[a] Department of Chemical Sciences, Faculty of Natural Sciences, Redeemer's University, Ede, Osun State, Nigeria
[b] Department of Biochemistry, Faculty of Basic Medical Sciences, Redeemer's University, Ede, Osun State, Nigeria

ARTICLE INFO

Article history:
Received 20 December 2020
Revised 14 October 2021
Accepted 20 October 2021

Editor: DR B Gyampoh

Keywords:
Albino rat
Atherosclerosis
Cellulose
Hibiscus sabdariffa
Histology

ABSTRACT

Despite the several applications of modified cellulose, there is limited information on their safety, and antidyslipidemic functions, which are the focus of this study. To address this, cellulose isolated from *Hibiscus sabdariffa* cellulose was surface modified using nitrilotriacetic acid to produce nitrilotriacetic acid modified *Hibiscus sabdariffa* cellulose (HSNT). It was characterized using Fourier transformed infrared spectroscopy (FTIR), X-ray diffraction (XRD), thermogravimetric (TGA) analysis, scanning electron microscopy (SEM) and carbon, hydrogen, nitrogen, sulfur/oxygen (CHNS/O) analyzer. The study further investigated the safety of HSNT at the doses of 50, 100, and 150 mg kg^{-1} body weight in albino rats after a 7-day uninterrupted oral gavage. Histology of cardiac and hepatic tissues was observed, in addition to estimation of clinico-biochemical parameters such as atherogenic index of plasma (AIP), Castelli's risk index (CRI-1), total cholesterol, high-density lipoprotein cholesterol (HDL-C), triglyceride (TG), albumin (ALB), aspartate aminotransferase (AST) and alanine aminotransferase (ALT). FTIR revealed peaks corresponding to the synthesis of HSNT, while XRD showed HSNT to have a crystallinity index of 53.20% with a type I cellulose crystal. HSNT had no significant effect on the absolute heart and liver weights, heart and liver organo-somatic indices, TG, AST, and ALB. Exposure to HSNT-50 caused a significant decrease in AIP levels. However, administration of HSNT-100 and 150 significantly reduced ALT, total cholesterol, and CRI-1 levels but caused a significant elevation in HDL-C levels. Cardiac histology revealed mild inflammatory and fatty infiltration of the myocardium, while the significant indications of the hepatic morphology included congestion of vessels and mild focal periportal infiltration at the HSNT-100 and HSNT-150 doses. Our preliminary data seem to indicate the potential of HSNT modification to resolve blood lipid abnormalities and make a case for an expanded study on its cardio-hepatic effects as well as study to understand the causes of congestion in hepatic vessels.

* Corresponding author.
E-mail address: walexy62@yahoo.com (A. Adewuyi).

https://doi.org/10.1016/j.sciaf.2021.e01025

Introduction

Cellulose is a polysaccharide consisting of $\beta-1,4$-glycosidic linked D-glucose units with the general formula $(C_6H_{10}O_5)n$. It is hydrophilic, soluble in some organic solvents and biodegradable with a chiral structure. Cellulose has unique properties such as crystallinity, biodegradability, hydrophobicity, tensile and compressive strength, which grants its application in different fields of research [1]. These properties can be improved by a simple modification to form derivates of cellulose such as hydroxyethyl, hydroxypropylmethyl, ethyl, sodium carboxymethyl, hydroxypropyl, methyl and carboxymethyl cellulose [2]. Cellulose is a unique resource in terms of structure and properties. It can serve as starting materials for other useful products due to the ease of the physical and chemical process of modification, which improves on its performance, especially the microstructured architectures, which places modified cellulose as a promising and broadly applicable material in several applications [3]. It exhibits low energy conformation due to its D-glucopyranose ring units chair configuration, which is linked by $\beta-1,4$-glycosidic bonds. Being a polymer, each of its anhydroglucose unit contains three reactive hydroxyl functional groups within its chain, which are positioned in its ring plane. The primary hydroxyl functional group is located at C6 while the secondary hydroxyl functional groups are located at C2 and C3 [1]. It is a linear homopolysaccharide and capable of forming extensive intra and intermolecular hydrogen bonds [4]. The hydroxyl functional groups are mostly involved in the modifications [5] with reaction, which includes esterification, sulphorization, amidation, oxidation, etherification, halogenation and urethanization [6].

One of the common derivatives or modified cellulose are the esterified cellulose. They are formed when cellulose reacts with a carboxylic acid. Cellulose esters have found several applications in many industries like food, paper, pharmaceutical, textile, and cosmetics [7]. They have been used in different types of pharmaceuticals such as drug delivery and control, bioadhesives, tableting of drugs, thickening agent, stabilizers, binders, fillers, and gelling agents [8–10]. Despite the several pharmaceutical applications of cellulose esters, there is limited information on its safety, atherogenic, and cardiac effects, which is the focus of this study. Although there are no harmful effects reported for the use of cellulose, there is no confirmation either of the safety or atherogenic effect of its modified form. However, its effect will depend on the type of modification the cellulose is subjected to, which makes it necessary to check the effect of such modified cellulose on clinical indices.

Atherosclerosis, oxidative stress, and hyperlipidemia are risk factors associated with cardiovascular diseases [11], which is responsible for millions of death annually [12]. Dyslipidemia is an abnormal or unhealthy amount of lipid in the blood system. It is characterized by a low level of high-density cholesterol lipoprotein and high levels of total cholesterol, triglycerides, and the low-density cholesterol lipoprotein [13, 14]. These characteristics contribute to the development of atherosclerosis, which can be correlated with the magnitude of cardiovascular risks. Thus, finding a means to reduce the risk of cardiovascular diseases which are increasing in both developed and developing countries with focus on an antidyslipidemic agent. Although several synthetic therapies have been developed, they are expensive and have reported varied side effects [15], which necessitates the search for cheaper and effective plant-based product that is from a renewable source. The use of modified cellulose may serve this purpose in controlling the risk of cardiovascular diseases as they may exhibit antidyslipidemic functions due to the possibility of introducing different functional groups to it. However, to the best of our knowledge, there are no currently reported studies on its atherogenic or cardiovascular functions. The present study, therefore, investigated the safety, cardiac, and atherogenic effects of nitrilotriacetic acid modified cellulose in albino rats.

Materials and methods

Materials

The seeds of *Hibiscus sabdariffa* obtained from a garden in the University of Ibadan, identified at the Department of Botany and Microbiology, University of Ibadan. They were ground in an industrial mill, extracted with n-hexane in order to defat it and air-dried. Nitrilotriacetic acid, acetic acid, sodium hydroxide, chloroacetylchloride, sodium chlorite, and all other chemicals used in this study were from Sigma-Aldrich (Brazil). Diagnostic kits (Randox Crumlin, UK) were used in the assays involving HDLC, total cholesterol, TG, AST, ALT, and albumin. Other general reagents were supplied by Sigma Company (USA).

Isolation and modification of cellulose from the seed of hibiscus sabdariffa

Cellulose was isolated from *Hibiscus sabdariffa* as previously reported [5] using 500 g of the defatted *Hibiscus sabdariffa* seed. The isolated cellulose (10 g) was poured into a three-neck round bottom flask containing chloroacetylchloride. The mixture of cellulose and chloroacetylchloride was stirred at 80 °C for 2 h. Nitrilotriacetic acid (3 g) was added and refluxed under continuous stirring for 5 h. The product formed was cooled to room temperature, distilled water added, and centrifuged at 5500 rpm for 10 min. This step was repeated three more times using distilled water to remove excess nitrilotriacetic acid. HSNT formed was dried overnight in the oven set at 50 °C to give a product yield of 94.97%.

Characterization

HSNT was blended with KBr in a pellet and analyzed for functional groups using FTIR (Perkin Elmer, Spectrum RXI 83,303) in the range of 400 - 4500 cm^{-1} while the elemental composition was evaluated using Perkin Elmer Series II CHNS/O analyzer (Perkin Elmer, 2400, USA). The X-ray diffraction pattern was measured on an X-ray diffractometer (XRD-7000X-Ray diffractometer, Shimadzu). The crystallinity index (I_c) was determined using the height of 200 peaks (I_{002}, $2\theta = 22.5°$) and the minimum intensity between the 200 and 110 peaks (I_{AM}, 2θ=18°) expressed as:

$$I_c(\%) = \left(\frac{I_{002} - I_{AM}}{I_{002}}\right) \times 100 \quad (1)$$

where I_{002} represents both crystalline and amorphous material, while I_{AM} represents the amorphous material only. The PSD and zeta potentials were analyzed using a zeta potential analyzer (DT1200, Dispersion technology) at 25 °C. TGA was measured using a simultaneous DTA-TG apparatus (SHIMADZU, C30574600245). The surface area was measured as BET surface area, and surface morphology was analyzed on micrograph using SEM (JEOL JSM-6360LV, Japan).

Water holding, oil holding, and swelling capacity

Water holding capacity (WC) was determined, as previously reported [16]. This was achieved using 0.5 g (X_1) of sample dispersed in 10 mL of distilled water in a pre-weighed, clean centrifuge tube (X), and spinned at 4000 rpm for 15 min. The weight of the centrifuge tubes with the distilled water-soaked samples (X_2) was recorded after the removal of the supernatant. WC was estimated as:

$$WC\ \left(gg^{-1}\right) = \frac{(X_2 - (X + X_1)}{X_1} \quad (2)$$

Oil holding capacity (OC) was determined as previously described [17] by weighing 0.1 g (W) of HSNT into a calibrated centrifuge tube containing 5 mL (V_1) of *Picralima nitida* seed oil. This was stirred continuously for 10 min and centrifuged at 5000 rpm for 30 min. The supernatant *Picralima nitida* oil (V_2) was removed, and the absorbed oil was calculated as:

$$OC\ \left(mLg^{-1}\right) = \frac{V_1 - V_2}{W} \quad (3)$$

HSNT was further analyzed for its swelling capacity (SC) by a process previously reported [18]. It involved weighing 0.5 g (W) of HSNT in a calibrated tube and measuring its initial bed volume (V_1). This was mixed with 10 mL deionized, shaken vigorously and placing it in water bath at 25 °C for 24 h. The final volume (V_2) measured and the swelling capacity estimated as:

$$SC\ \left(mLg^{-1}\right) = \frac{V_2 - V_1}{W} \quad (4)$$

Heavy metal adsorption capacity

The metal uptake capacity of HSNT towards Ni^{2+}, Pb^{2+}, Cu^{2+} and Cd^{2+} ions was evaluated using nickel nitrate ($Ni(NO_3)_2$•$6H_2O$), lead nitrate ($Pb(NO_3)_2$), copper sulfate ($Cu(SO_4).5H_2O$) and cadmium sulfate ($3CdSO_4$•$8H_2O$) salts. The uptake capacity was achieved by mixing 0.1 g of HSNT with 50 mL of different solutions of the metal ions at a concentration of 100 mg L^{-1} in beakers at 25 °C and 200 rpm for 3 h using an electric shaker. The resulting mixture was centrifuged at 5000 rpm for 10 min to separate the HSNT from the solution. The metal ion concentrations before and after the shaking were determined using Atomic Absorption Spectrometer (Varian AA240FS) and the metal ions adsorption capacity was calculated as:

$$q_e = \frac{(C_o - C_e)V}{M} \quad (5)$$

Where q_e is the adsorption capacity in mg g^{-1}, C_o and C_e are initial and final metal ion concentrations (mg L^{-1}), respectively, while M and V are weight (g) of HSNT and volumes (L) of metal ions solution.

Animals

Twenty adult male albino rats used in this study weighing between 160 and 190 g were purchased from the University of Ibadan animal house facility in Ibadan, Oyo State, Nigeria. The animals were transported in a well-ventilated vehicle to the Redeemer's University Animal House, where they were acclimated, fed ad libitum, and provided unrestricted access to tap water. All animals received humane care outlined by the University's Ethical Committee (RUN/BCH/13/5248).

Table 1
Water holding, oil holding and swelling capacities of HSNT.

Sample	Water holding capacity (g^{-1})	Oil holding capacity (mL g^{-1})	Swelling capacity (mL g^{-1})
HSNT	6.407 ± 001	5.296 ± 0.05	2.240 ± 0.02

Values are expressed as Mean ± SEM (3 replicates).

Experimental design

Albino rats were randomly divided into control and three treatment groups ($n = 5$) and orally administered with HSNT for seven consecutive days. The control group was administered normal saline while the treatment groups were administered with 50, 100, and 150 mg kg^{-1} HSNT, i.e., HSNT-50, HSNT-100, and HSNT-150, respectively. The doses and duration were selected based on previously reported studies [19, 20].

Preparation of samples, and estimation of selected clinical markers

After seven days of administering HSNT, the animals were fasted overnight and euthanized following a cervical dislocation procedure. Heart and liver were excised for histology while the plasma was used to assess clinical markers such as HDL-C, total cholesterol, TG, AST, ALT, and albumin. These biochemical variables were measured in plasma using a spectrophotometer (Bibby Scientific Jenway 7305 UV, UK) according to the manufacturer's specifications. The AIP was calculated as the 10 logarithm of the ratio of the concentration of TG to HDL-C, as previously described [21]. In addition, the CRI-1 was calculated as the ratio of TC to HDL-C [22]. The heart and liver organo-somatic indices (HOSI and LOSI) were calculated as:

$$Organo-somatic\ Indices = \frac{Absolute\ tissue\ weight}{Body\ weight} \times 100 \quad (6)$$

Histological studies

The histology was carried out as previously described [23] with little modifications. Briefly, three representative samples of heart and liver tissues were harvested from each group and fixed in 10% formalin. The fixed tissues were subsequently dehydrated in ascending grades of alcohol (70%–100%), and embedded in paraffin using embedding rings. Blocks were placed at 4 °C for 15 min to solidify. Sections (≈5 µm) were cut using a Reichert-Jung rotary microtome, placed in water bath at a temperature of 45 °C for 10 min and then put on silinated slides. Slides were allowed to dry overnight in an 37 °C oven, and stained with haematoxylin and eosin. Specimens were then examined for histopathological changes with an Amscope microscope camera attached to an electrical light microscope.

Statistics

Data were captured as the mean ± standard error of the mean (with significance at $p<0.05$). Further analyses were performed using a one-way analysis of variance (ANOVA) and Dunnet's *post hoc* test (Version 8: Graph Pad Prism software, Inc., San Diego, CA).

Results

Synthesis and characterization of HSNT

Fig. 1a showed peaks corresponding to the different functional groups present on the synthesized HSNT. Fig. 1b revealed a crystallinity index of 53.20% for HSNT. As presented in Fig. 1c, HSNT exhibited potential ranging from 0.00 to −3.00 mV. The CHNS/O analysis revealed a carbon content of 49.35%, hydrogen of 9.84%, and nitrogen of 3.03%. The surface area was found to be 10.00 m^2g^{-1} (Fig. 1d). The particle size distribution of HSNT was found to be monomodal, with mean size of 0.171 (Fig. 2a) and being homogeneous and flaky on the surface (Fig. 2b). The thermal degradation pattern is shown in Fig. 2c with four degradation stages of mass loss. The metal adsorption capacity of HSNT towards some selected metals ions (Pb^{2+}, Cu^{2+}, $Ni^{2+,}$ and Cd^{2+}) is presented in Fig 2d. HSNT demonstrated the highest adsorption capacity and percentage removal towards Pb^{2+}ions. Table 1 expressed the capacities of HSNT to uphold polar and non-polar molecules.

Effect of HSNT on absolute organ weights, organo-somatic indices, and plasma total protein

The organs of the albino rats increased after the feeding period when compared to the control (Table 2). The highest heart (0.69 ± 0.04 g) and liver (6.23 ± 0.40 g) weights were recorded for HSNT-50. However, there was no significant difference in the values obtained.

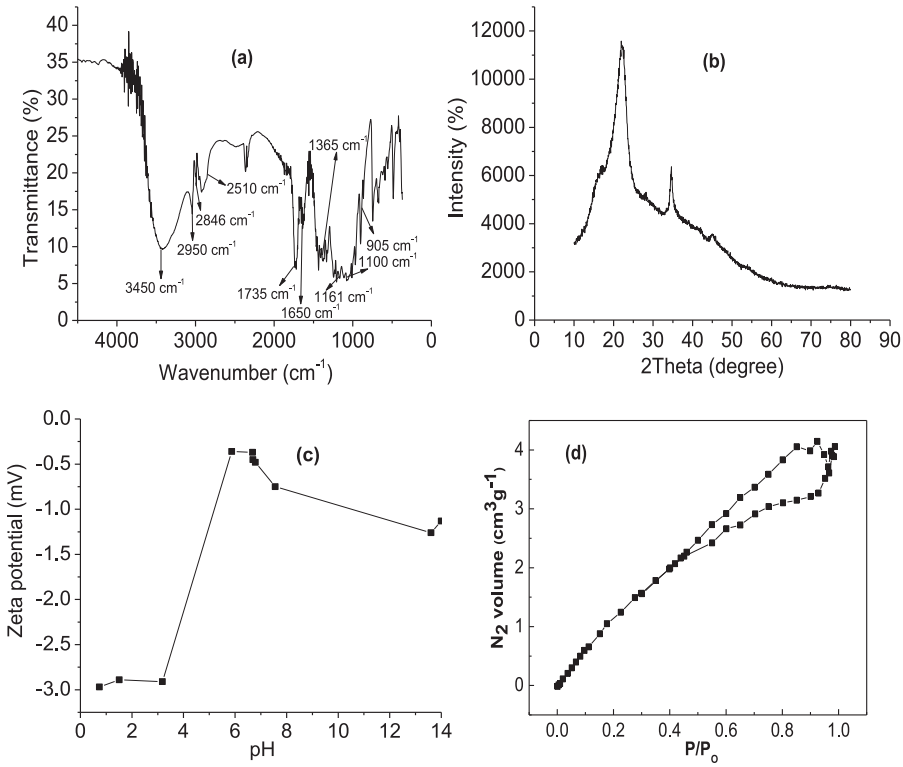

Fig. 1. FTIR (a), XRD (b), Zeta potential (c) and BET surface area (d) of HSNT.

Table 2
Absolute organ weights, organo-somatic indices and plasma total protein levels of Albino rats fed with HSNT.

	Control	HSNT-50	HSNT-100	HSNT-150
Heart (g)	0.55 ± 0.04	0.69 ± 0.04	0.57 ± 0.02	0.68 ± 0.09
HOSI	0.30 ± 0.04	0.69 ± 0.02	0.30 ± 0.01	0.28 ± 0.03
Liver (g)	4.60 ± 0.50	6.23 ± 0.40	5.31 ± 0.34	5.94 ± 0.99
LOSI	0.29 ± 0.03	0.32 ± 0.02	0.30 ± 0.01	0.28 ± 0.03
Total protein (mg g $^{-1}$)	2.75 ± 0.04	3.10 ± 0.20	2.81 ± 0.16	2.95 ± 0.12

Values are expressed as Mean ± SEM (n = 5).
HOSI = Heart organo-somatic indices.
LOSI = Liver organo-somatic indices.
HSNT-50 = Treatment group fed with nitrilotriacetic acid modified *Hibiscus sabdariffa* cellulose at 50 mg kg^{-1}.
HSNT-100 = Treatment group fed with nitrilotriacetic acid modified *Hibiscus sabdariffa* cellulose at 100 mg kg^{-1}.
HSNT-150 = Treatment group fed with nitrilotriacetic acid modified *Hibiscus sabdariffa* cellulose at 150 mg kg^{-1}.

Effect of HSNT on tradition and non-traditional lipid parameters

Treatment of rats with HSNT did not significantly alter the TG levels when compared with the control groups (Fig. 3), however, HSNT-100 and HSNT-150 significantly depleted the total cholesterol levels while concomitantly elevating the HDL-C levels. Furthermore, a significant decrease in AIP levels was observed at the HSNT-50 treatment, but for the CRI-1 ratio, a decline was observed at the higher doses of 100 and 150 mg kg^{-1} of HSNT (Fig. 4)

Effect of HSNT on hepatic function indices

Administration of HSNT to rats at all treatment doses elicited a non-significant decrease in AST and ALT levels compared to control (Fig. 5). The least reduction in ALT level was found at dose HSNT-150.

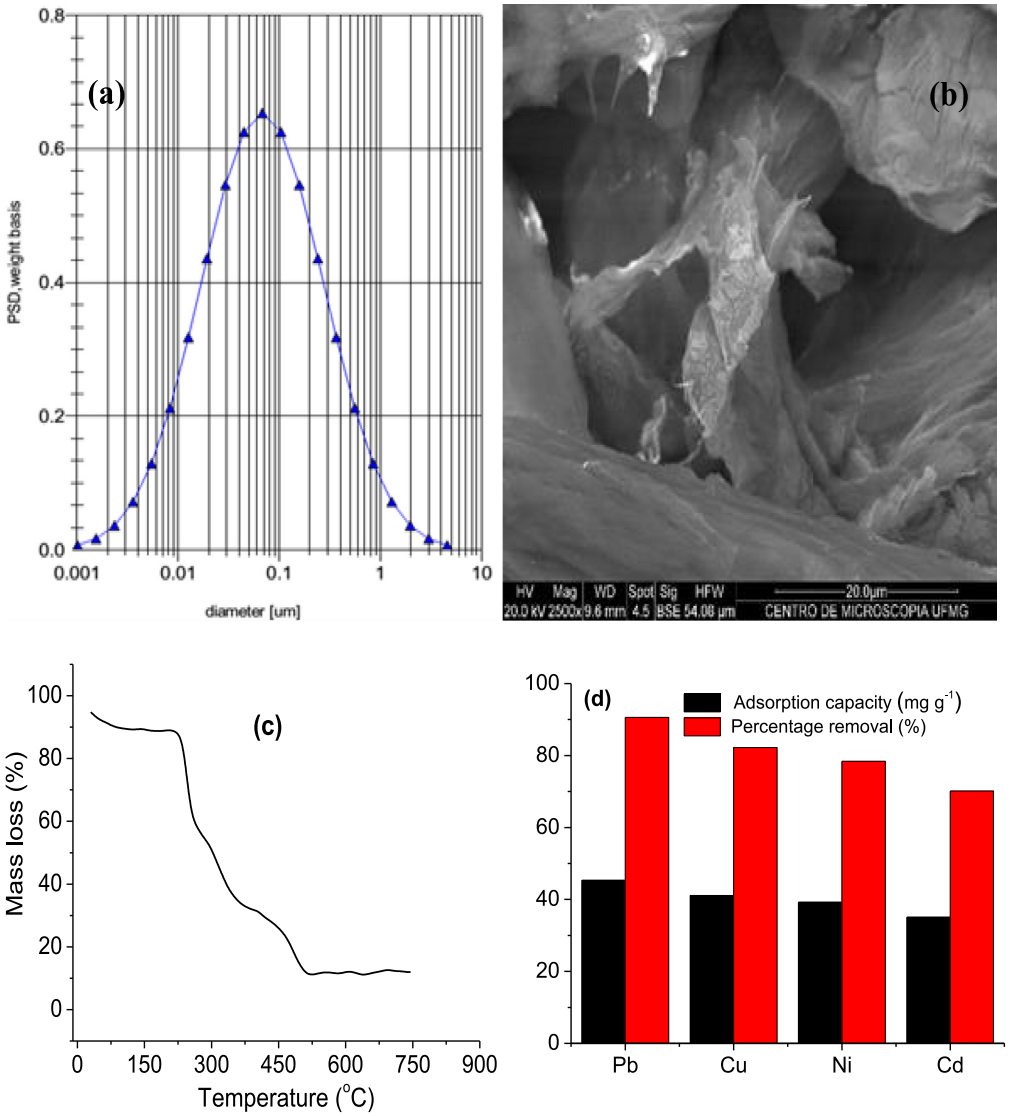

Fig. 2. PSD (a), SEM (b), TG (c), adsorption capacity and metal percentage removal (d) of HSNT.

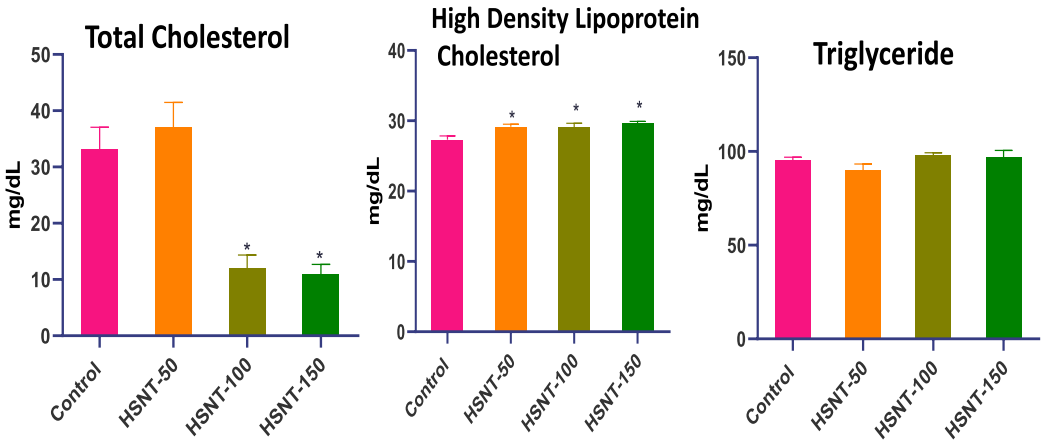

Fig. 3. Effect of HSNT on traditional lipid profile parameters in rats. Values are expressed as mean ±SEM ($n = 5$). * Significantly different from control ($p<0.05$).

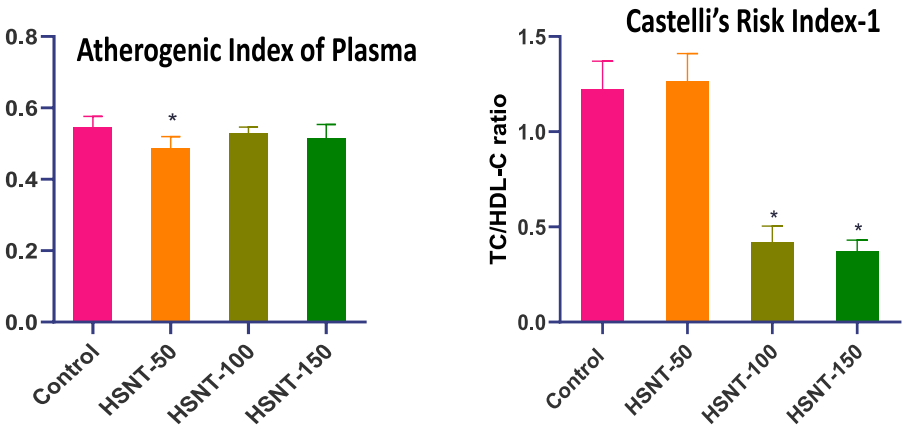

Fig. 4. Effect of HSNT on non-traditional lipid profile parameters in rats. Values are expressed as mean ±SEM ($n = 5$). * Significantly different from control ($p<0.001$).

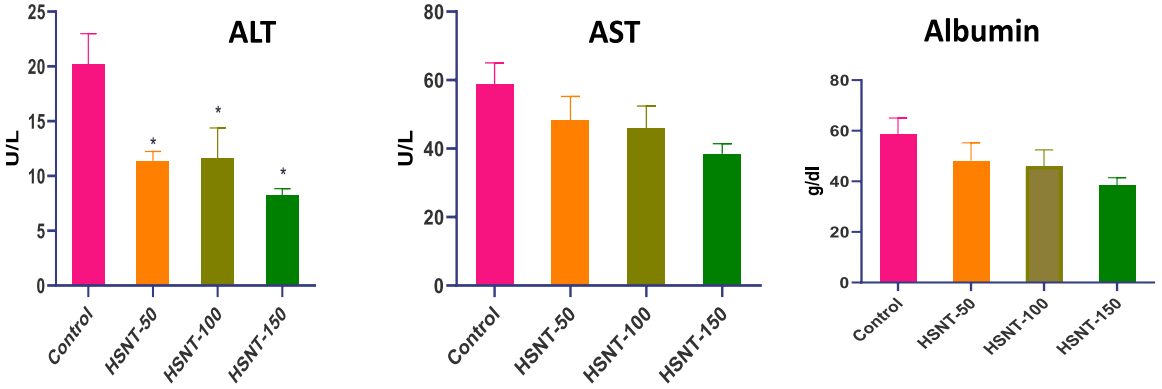

Fig. 5. Effect of HSNT on hepatic function markers in rats. Values are expressed as mean ±SEM ($n = 5$). * Significantly different from control ($p<0.05$), ALT = Alanine aminotransferase, AST = Aspartate aminotransferase.

Effect of HSNT on the cardiac and hepatic histology of rats

The results showed mild infiltration of myocardium with inflammatory cells in HSNT 100 and 150 group (Fig. 6a and 6b). On the other hand, the liver of rats in the control and HSNT-50 groups presented normal-looking morphology, while those treated with HSNT-100 and HSNT-150 showed periportal infiltration as well as congestion of blood vessels (Fig. 6b).

Discussion

The FTIR revealed peaks at 3450 and 2950, which may be assigned to frequencies of hydroxyl and alkane functional groups, respectively. The presence of the hydroxyl functional groups suggests that the modification reaction occurred in the amorphous region, while the hydroxyl group in the crystalline regions were untouched [24]. The peak at 1735 cm^{-1} was attributed to the ester carbonyl group formed as a result of the reaction between the hydroxyl functional group on the cellulose and the carboxylic acid group of the nitrilotriacetic acid. The ester functional group of HSNT may probably be responsible for the biofunction exhibited by HSNT in this study. The peak at 2846 and 1365 cm^{-1} were attributed to C–H stretching and bending vibration of C–O bonds in the polysaccharide aromatic rings, respectively. The peak found at 1650 cm^{-1} was attributed to the unreacted carboxylic acid group from nitrilotriacetic acid on the surface of the cellulose. Peaks at 1161 and 1100 cm^{-1} were accounted as being peaks from C–O-C stretching of lignin and C–O vibrational stretching of cellulose, respectively. A peak, observed at 1025 cm^{-1}, was assigned to the C–O-C pyranose ring stretching vibration while the peak at 905 cm^{-1} was attributed to the stretching at β-(1→4) glycosidic linkages.

The XRD diffractogram of HSNT revealed a pattern, attributed to that of a typical of cellulose I crystal [17]. The zeta potential increased with pH, which later reduced at pH 6. The potential distribution at the surface of HSNT showed that the material is stable in liquid medium [25]. The zeta potential is also an indication of the surface charge of HSNT [26]. The CHN analysis confirmed the elemental composition of HSNT to be carbon, hydrogen, and nitrogen. The surface area is small with particle size distribution, with the SEM image revealing its surface as homogeneous. Thermal degradation

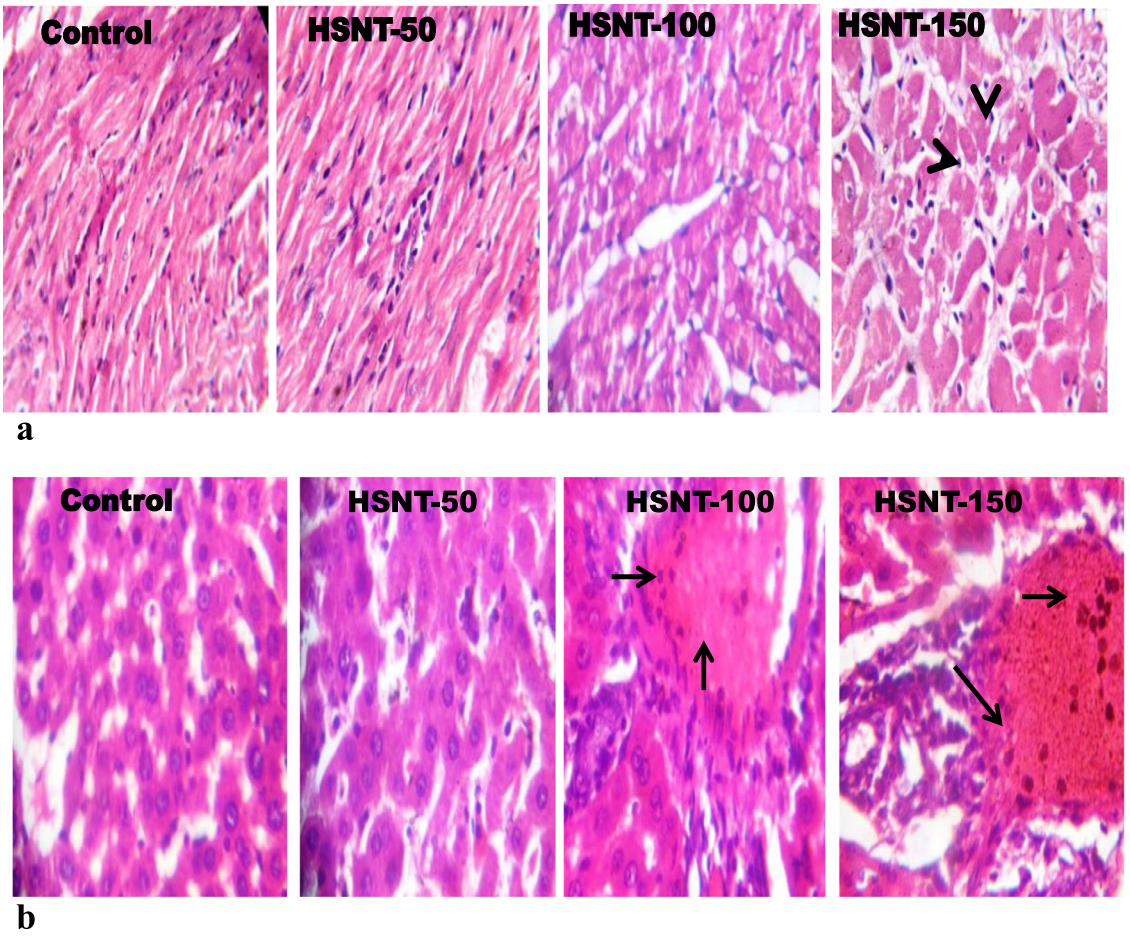

Fig. 6. (a): Representative photomicrographs of the heart showing normal-looking myocardium in control, HSNT-50 and HSNT 100 groups. Rats treated HSNT-150 showed mild infiltration of the myocardium with inflammatory cells (arrowed). Haematoxylin and Eosin staining, Magnification 400 X, (**b**): Representative photomicrographs of the liver showing normal-looking morphology in control and HSNT-50 groups. Rats treated HSNT-100 and HSNT-150 animals fed with HSNT100 and HSNT-150 presented with congestion of vessels (short arrows) and focal periportal infiltration (long arrow). Haematoxylin and Eosin staining, Magnification 400 X, HSNT-50 = Treatment group fed with nitrilotriacetic acid modified *Hibiscus sabdariffa* cellulose, at 50 mg kg^{-1}, HSNT-100 = Treatment group fed with nitrilotriacetic acid modified *Hibiscus sabdariffa* cellulose, at 100 mg kg^{-1}, HSNT-150 = Treatment group fed with nitrilotriacetic acid modified *Hibiscus sabdariffa* cellulose, at 150 mg kg^{-1}.

revealed an initial loss at a temperature range of between 65 °C and 150 °C, which may be attributed to the loss of water molecules in HSNT. Possibly, loss of volatile molecules might have taken place also at this temperature. The second stage of degradation occurred at 150–350 °C, which was accounted for as being the degradation leading to the formation of 1,4 and 1,6 anhydroglucopyranoside while the third stage took place at 350–460 °C, which was assigned to the depolymerization at 1,4 glycosidic bond [27]. The last stage involved pyrolysis to lower molecules and the loss of lignin and char [28].

HSNT showed high adsorption capacity preference towards Pb^{2+} (45.30 mg g^{-1}) while the least capacity was expressed towards Cd^{2+} (35.05 mg g^{-1}). Cu was 41.10 mg $g^{-1,}$ and capacity towards Ni was 39.20 mg g^{-1}. The percentage removal was in the range Pb^{2+} (90.60%) > Cu^{2+} (82.20%) > Ni^{2+} (78.40%) > Cd^{2+} (70.10%). The swelling capacity is the expression of the amount of water that HSNT can absorb. The ability of HSNT to hold water molecules may be attributed to the presence of a hydroxyl group in its molecule. The water holding capacity may be due to the ability of the hydroxyl group to undergo hydrogen bonding with the water molecules, which may suggests its possibility of being absorbed in biological system like when fed into rat. The water holding capacity of HSNT was found to be 6.407 ± 001 g^{-1}. The oil holding capacity of HSNT relates to the amount of oil it can retain per unit weight. This is also an indication of its interactive capacity with non-polar molecules. In the case of HSNT, the value was 5.296 ± 0.05 mL g^{-1}. The swelling was found to be 2.240 ± 0.02 mL g^{-1}.

There were no observable treatment-induced adverse effects on animals in the course of the study. Moreover, the absolute weights and heart and liver organo-somatic indices were not significantly altered by the administration of HSNT. Although HSNT did not alter TG levels significantly, its presence lowers the total cholesterol levels at HSNT-100 and HSNT-150 significantly. Usually, an increase or decrease in TG and total cholesterol occur when there are abnormalities in the degradation, synthesis, and transport of their associated lipoprotein particles[29]. Several epidemiologic studies [29–32] have

linked changes in TG and total cholesterol to atherosclerotic cardiovascular diseases and other coronary heart diseases. The recorded significant decrease in the total cholesterol level is an indication that HSNT may be useful in managing hyperlipoproteinemia. The reduced levels of total cholesterol further suggest that HSNT might serve as a protective factor against the development of the atherosclerotic cardiovascular disease. The decrease in HDL-C levels further supports the suggestion that HSNT may be useful in the management of hyperlipoproteinemia.

Studies have successfully reported the use of AIP as an index for assessing cardiovascular risk factors [33,34]. The current AIP values of HSNT suggests a fair risk factor [35]. Furthermore, the CRI-1 may be used to predict the prevalence of a predisposition of cardiovascular risk [36]. The index indicated a major significant difference when the control group was compared with groups fed with 100 and 150 mg kg^{-1} of HSNT. Studies have shown that a low-fat meal may help reduce ALT [37]. The significant reduction in ALT may be attributed to the fat-reducing ability of HSNT. The reduced ALT value further corroborates its ability to reduce total cholesterol. This is an indication that HSNT may be a protective factor that may help reduce ALT levels. Previous studies have also reported the consumption of coffee as a protective factor [38,39] in this regard. Most plant extracts that have shown prospects as protective agents for elevated ALT are not pure molecules but a mixture of naturally occurring molecules. However, HSNT is pure, it was produced from purely isolated cellulose from *Hibiscus sabdariffa* and during production of HSNT we ensured that no undesired residue was included in it; however, it can function as a single molecule with a unique identity with promising protective factors for elevated ALT.

Histological observations of the heart following the administration of different doses of HSNT revealed no significant lesions in control, HSNT-50, and HSNT 100 groups. Similar observation has been reported for the use of exopolysaccharide isolated from *Bacillus subtilis* on cardiovascular diseases and atherogenic indices in rats [39]. However, mild infiltration of the myocardium at the highest dose of HSNT-150 was observed. In a similar trend, there were no observable histological distortions in the hepatic morphology of rats in control and HSNT-50 groups. Contrariwise, animals fed with HSNT-100 and HSNT-150 presented with congestion of vessels, mild steatosis, and focal periportal infiltration. It might be difficult to conclude in clear terms on what may be attributed to the contrary observation; however, it is necessary to further study the cardio-hepatic effects of HSNT in future studies.

Conclusion

The administration of HSNT in albino rats significantly elevated HDL-C without significant organ damage at low doses, while ALT was significantly reduced. The photomicrographs revealed no significant lesions in control, HSNT-50, and HSNT 100 groups. This study hence provides preliminary pre-clinical data on the safety profile of HSNT.

Declaration of Competing Interest

The authors declare that they have no known competing financial interests or personal relationships that could have appeared to influence the work reported in this paper.

CRediT authorship contribution statement

Adewale Adewuyi: Conceptualization, Methodology, Investigation, Data curation, Writing – original draft, Supervision, Validation, Writing – review & editing. **Chiagoziem A. Otuechere:** Conceptualization, Methodology, Investigation, Data curation, Writing – original draft, Supervision, Validation, Writing – review & editing. **Olusegun L Adebayo:** Visualization, Investigation. **Mmachukwu Oyeka:** Data curation, Software. **Caleb Adewole:** Data curation, Software.

Acknowledgment

Authors are grateful to the Department of Chemistry, Federal University of Minas Gerais, Brazil for the analysis of cellulose.

References

[1] S.F. Kabir, et al., Cellulose-based hydrogel materials: chemistry, properties and their prospective applications, Prog Biomater 7 (3) (2018) 153–174.
[2] M.L. Bruschi, et al., in: Nanostructured Therapeutic Systems With Bioadhesive and Thermoresponsive properties, in Nanostructures for Novel Therapy, Elsevier, 2017, pp. 313–342.
[3] T. Heinze, in: Cellulose: Structure and properties, in Cellulose chemistry and properties: fibers, Nanocelluloses and Advanced Materials, Springer, 2015, pp. 1–52.
[4] H.T. Sahin, M.B. Arslan, A study on physical and chemical properties of cellulose paper immersed in various solvent mixtures, Int. J. Mol. Sci. 9 (1) (2008) 78–88.
[5] A. Adewuyi, F.V. Pereira, Isolation and surface modification of cellulose from underutilized Luffa cylindrica sponge: a potential feed stock for local polymer industry in Africa, J. Ass. Arab Univ. Basic Appl. Sci. 24 (1) (2017) 39–45.
[6] Y. Habibi, Key advances in the chemical modification of nanocelluloses, Chem. Soc. Rev. 43 (5) (2014) 1519–1542.
[7] R. Khiari, M. Belgacem, in: Potential for Using Multiscale Posidonia oceanica waste: Current status and Prospects in Material science, in Lignocellulosic Fibre and Biomass-Based Composite Materials, Elsevier, 2017, pp. 447–471.
[8] A. Ludwig, The use of mucoadhesive polymers in ocular drug delivery, Adv. Drug Deliv. Rev. 57 (11) (2005) 1595–1639.
[9] S. Movassaghian, et al., Development of amitriptyline buccoadhesive tablets for management of pain in dental procedures, Drug Dev. Ind. Pharm. 37 (7) (2011) 849–854.

[10] J. Shokri, K. Adibkia, Application of cellulose and cellulose derivatives in pharmaceutical industries, Cellulose-medical, Pharmaceutical And Electronic Applications, IntechOpen, 2013.
[11] C. Li, et al., Cholesteryl ester transfer protein inhibitors in the treatment of dyslipidemia: a systematic review and meta-analysis, PLoS One 8 (10) (2013) e77049.
[12] N. Fidèle, et al., Hypolipidemic, antioxidant and anti-atherosclerogenic effect of aqueous extract leaves of Cassia. occidentalis Linn (Caesalpiniaceae) in diet-induced hypercholesterolemic rats, BMC Complement. Altern. Med. 17 (1) (2017) 76.
[13] J.E. Hokanson, M.A. Austin, Plasma triglyceride level is a risk factor for cardiovascular disease independent of high-density lipoprotein cholesterol level: a metaanalysis of population-based prospective studies, J. Cardiovasc. Risk 3 (2) (1996) 213–219.
[14] L. Schwingshackl, G. Hoffmann, Systematic review and meta analysis, Br. J. Nutr. 111 (2014) 2047–2058.
[15] S. Devi, R. Singh, Assessment of lipid lowering effect of Nepeta hindostana herb extract in experimentally induced dyslipidemia, J. Nutr. Intermed. Metabol. 9 (2017) 17–23.
[16] M. Zhang, C.-j. Zhang, S. Shrestha, Study on the preparation technology of superfine ground powder of Agrocybe chaxingu Huang, J. Food Eng. 67 (3) (2005) 333–337.
[17] H. Lu, et al., Morphological, crystalline, thermal and physicochemical properties of cellulose nanocrystals obtained from sweet potato residue, Food Res. Int. 50 (1) (2013) 121–128.
[18] E. Lecumberri, et al., Dietary fibre composition, antioxidant capacity and physico-chemical properties of a fibre-rich product from cocoa (Theobroma cacao L.), Food Chem. 104 (3) (2007) 948–954.
[19] A. Adewuyi, et al., Renal toxicological evaluations of sulphonated nanocellulose from Khaya sengalensis seed in Wistar rats, Chem. Biol. Interact. 284 (2018) 56–68.
[20] C. Otuechere, et al., In vivo hepatotoxicity of chemically modified nanocellulose in rats, Hum. Exp. Toxicol. 39 (2) (2020) 212–223.
[21] T.-T. Wu, et al., Atherogenic index of plasma (AIP): a novel predictive indicator for the coronary artery disease in postmenopausal women, Lipids Health Dis. 17 (1) (2018) 197.
[22] A.A. Kamoru, et al., Castelli risk index, atherogenic index of plasma, and atherogenic coefficient: emerging risk predictors of cardiovascular disease in HIV-treated patients, Saudi J. Med. Pharmaceut. Sci. (2017) 1101–1110.
[23] M. Slaoui, L. Fiette, in: Histopathology procedures: from Tissue Sampling to Histopathological evaluation, in Drug safety Evaluation, Springer, 2011, pp. 69–82.
[24] D. Roy, J.T. Guthrie, S. Perrier, Graft polymerization: grafting poly (styrene) from cellulose via reversible addition− fragmentation chain transfer (RAFT) polymerization, Macromolecules 38 (25) (2005) 10363–10372.
[25] B. Salopek, D. Krasic, S. Filipovic, Measurement and application of zeta-potential, Rudarsko-geolosko-naftni zbornik 4 (1) (1992) 147.
[26] B.J. Kirby, Micro-and Nanoscale Fluid mechanics: Transport in Microfluidic Devices, Cambridge university press, 2010.
[27] R.K. Sharma, A study in thermal properties of graft copolymers of cellulose and methacrylates, Adv. Appl. Sci. Res. 3 (6) (2012) 3961–3969.
[28] M.E. Babiker, et al., Pyrolysis characteristics of Phoenix dactylifera date palm seeds using thermo-gravimetric analysis (TGA), Int. J. Environ. Sci. Develop. 4 (5) (2013) 521.
[29] R.A. Cox, M.R. García-Palmieri, Cholesterol, triglycerides, and associated lipoproteins, Clinical Methods: the History, Physical, and Laboratory Examinations, 1990.
[30] I. Markaki, et al., High cholesterol levels are associated with improved long-term survival after acute ischemic stroke, J. Stroke Cerebrovasc. Dis. 23 (1) (2014) e47–e53.
[31] W. Zhao, et al., Low total cholesterol level is the independent predictor of poor outcomes in patients with acute ischemic stroke: a hospital-based prospective study, BMC Neurol. 16 (1) (2016) 36.
[32] S.R. Gnanenthiran, et al., Low total cholesterol is associated with increased major adverse cardiovascular events in men aged≥ 70 years not taking statins, Heart 106 (9) (2020) 698–705.
[33] M.H. Tan, D. Johns, N.B. Glazer, Pioglitazone reduces atherogenic index of plasma in patients with type 2 diabetes, Clin. Chem. 50 (7) (2004) 1184–1188.
[34] U. Nwagha, et al., Atherogenic index of plasma as useful predictor of cardiovascular risk among postmenopausal women in Enugu, Nigeria, Afr. Health Sci. 10 (3) (2010).
[35] M. Dobiasova, AIP–atherogenic index of plasma as a significant predictor of cardiovascular risk: from research to practice, Vnitr. Lek. 52 (1) (2006) 64–71..
[36] M.A. Olamoyegun, R. Oluyombo, S.O. Asaolu, Evaluation of dyslipidemia, lipid ratios, and atherogenic index as cardiovascular risk factors among semi-urban dwellers in Nigeria, Ann. Afr. Med. 15 (4) (2016) 194.
[37] F. Shidfar, et al., The effects of extra virgin olive oil on alanine aminotransferase, aspartate aminotransferase, and ultrasonographic indices of hepatic steatosis in nonalcoholic fatty liver disease patients undergoing low calorie diet, Can. J. Gastroenterol. Hepatol. (2018) 2018.
[38] K.G. Lee, A. Mitchell, T. Shibamoto, Antioxidative activities of aroma extracts isolated from natural plants, Biofactors 13 (1–4) (2000) 173–178.
[39] C.E. Ruhl, J.E. Everhart, Coffee and caffeine consumption reduce the risk of elevated serum alanine aminotransferase activity in the United States, Gastroenterology 128 (1) (2005) 24–32.